JOURNAL OF VIROLOGY, Aug. 2005, p. 9449–9457 Vol. 79, No. 15
0022-538X/05/$08.00+0 doi:10.1128/JVI.79.15.9449–9457.2005

Human T-Lymphotropic Virus Type 1 Mitochondrion-Localizing Protein p13^{II} Sensitizes Jurkat T Cells to Ras-Mediated Apoptosis

Hajime Hiraragi,[1] Bindhu Michael,[1]† Amrithraj Nair,[1]† Micol Silic-Benussi,[2] Vincenzo Ciminale,[2] and Michael Lairmore[1,3,4]*

Center for Retrovirus Research and Department of Veterinary Biosciences, College of Veterinary Medicine,[1] Comprehensive Cancer Center,[3] and Department of Molecular Virology, Immunology, and Medical Genetics,[4] The Ohio State University, Columbus, Ohio, and Department of Oncology and Surgical Sciences, University of Padova, Padua 35128, Italy[2]

Received 7 October 2004/Accepted 18 April 2005

Human T-lymphotropic virus type 1 (HTLV-1) is the etiological agent of adult T-cell leukemia. In addition to typical retroviral structural and enzymatic gene products, HTLV-1 encodes unique regulatory and accessory proteins, including a singly spliced pX open reading frame II (ORF II) product, p13^{II}. We have demonstrated that proviral clones of HTLV-1 which are mutated in pX ORF II fail to obtain typical proviral loads and antibody responses in a rabbit animal model. p13^{II} localizes to mitochondria and reduces cell growth and tumorigenicity in mice, but its function in human lymphocytes remains undetermined. For this study, we analyzed the functional properties of Jurkat T cells expressing p13^{II}, using both transient and stable expression vectors. Our data indicate that p13^{II}-expressing Jurkat T cells are sensitive to caspase-dependent, ceramide- and FasL-induced apoptosis. p13^{II}-expressing Jurkat T cells also exhibited reduced proliferation when cultured at a high density. Furthermore, preincubation of the p13^{II}-expressing cells with a farnesyl transferase inhibitor, which blocks the posttranslational modification of Ras, markedly reduced FasL-induced apoptosis, indicating the participation of the Ras pathway in p13^{II}'s influence on lymphocyte survival. Our data are the first to demonstrate that p13^{II} alters Ras-mediated apoptosis in T lymphocytes, and they reveal a potential mechanism by which HTLV-1 alters lymphocyte proliferation.

Human T-lymphotropic virus type 1 (HTLV-1) is the etiological agent of adult T-cell leukemia/lymphoma (ATL), a highly aggressive T-cell malignancy characterized by circulating activated CD4$^+$ CD25$^+$ T cells (12). The virus is also associated with a variety of lymphocyte-mediated diseases, including HTLV-1-associated myelopathy/tropical spastic paraparesis (12, 16, 28). There are approximately 15 to 25 million HTLV-1-infected persons worldwide, and 3 to 5% of these infected subjects will develop HTLV-1-associated diseases (17). The underlying mechanism of virus-mediated lymphocyte transformation has been extensively investigated but is incompletely understood. Based on the long period of latency and the small percentage of individuals who develop ATL, the transformation of infected lymphocytes is believed to be initiated through the induction of cellular genes and alterations in cellular activation and death pathways by the viral proteins (28).

HTLV-1 is a member of the genus *Deltaretrovirus* of the family *Retroviridae*. The viral genome consists of long terminal repeats (LTRs) flanking genes encoding the structural and enzymatic proteins Gag, Pol, and Env. In addition, a region located between *env* and the 3′ LTR, pX, encodes the regulatory proteins Tax and Rex as well as several accessory proteins, namely, p12^{I}, p27^{I}, p13^{II}, and p30^{II} (1). The ability of HTLV-1 to produce these regulatory and accessory proteins through alternative splicing and selective codon usage classifies the virus among the complex retroviruses (4, 23). Recent studies have indicated a significant role for HTLV-1 accessory proteins in the life cycle of HTLV-1, particularly during the early phase of the viral infection of lymphocytes (1, 9, 16, 27, 30, 32, 40). Less is known, however, about the accessory protein p13^{II}, a singly spliced product of the second open reading frame (ORF II) of the pX gene region.

This protein selectively localizes to the inner membranes of mitochondria (5, 8) and directly binds to cellular protein farnesyl pyrophosphate synthetase (25). p13^{II} mRNA is expressed in various HTLV-1-infected cell lines isolated from clinical patients with ATL and HTLV-1-associated myelopathy/tropical spastic paraparesis, and circulating cytotoxic lymphocytes specific to ORF II products (i.e., p13^{II} and p30^{II}) have been detected in both HTLV-1-infected ATL patients and asymptomatic persons (3, 11, 31). Furthermore, although initial studies reported that HTLV-1 ORF II was dispensable for viral infection in vitro (14, 33), the selective ablation of pX ORF II protein expression encoded by infectious HTLV-1 proviral clones dramatically reduced viral infectivity and host humoral responses in rabbits (2, 37), indicating the requirement of the pX ORF II-encoded proteins, p13^{II} and p30^{II}, for natural HTLV-1 infection. In addition, we reported the suppressive effect of p13^{II} on both cell growth in vitro and tumorigenicity in a murine model (36). Collectively, these observations indi-

* Corresponding author. Mailing address: Department of Veterinary Biosciences, The Ohio State University, Columbus, OH 43210. Phone: (614) 292-4489. Fax: (614) 292-6473. E-mail: lairmore.1@osu.edu.

† Present address: Merck Research Laboratories, Merck & Co., Inc., Sumneytown Pike, P.O. Box 4, West Point, PA 19486-0004.

cate a distinct role for $p13^{II}$ in HTLV-1 infection and a potential role in HTLV-1-mediated lymphocyte transformation.

For this study, we used both transient and stable expression methods to test the effect of mitochondrion-localizing HTLV-1 $p13^{II}$ in Jurkat T cells in response to apoptotic stimuli. Annexin V staining assays indicated that the Jurkat T cells expressing $p13^{II}$ were more sensitive to apoptosis in a dose-dependent manner when treated with synthetic ceramide and Fas ligand (FasL), known apoptosis inducers of T lymphocytes. Furthermore, preincubation of $p13^{II}$-expressing Jurkat T cells with a farnesyl transferase inhibitor (FTI), which blocks the post-translational modification of Ras to its active form, resulted in a marked, dose-dependent protection against apoptosis, indicating the involvement of Ras-mediated signaling in the $p13^{II}$ alteration of lymphocyte responses to apoptotic stimuli. Our study is the first to demonstrate a role of the mitochondrion-localizing protein $p13^{II}$ of HTLV-1 in the lymphocyte response to Ras-mediated apoptosis, and it reveals a potential new mechanism for the HTLV-1-induced alteration of lymphocyte proliferation.

MATERIALS AND METHODS

Cells. Jurkat T cells (clone E6-1; American Type Culture Collection) were maintained in RPMI 1640 medium supplemented with 15% fetal bovine serum, 100 μg of streptomycin plus penicillin/ml, 2 mM L-glutamine, and 10 mM HEPES (cRPMI) (Invitrogen, Carlsbad, CA). 293T cells (American Type Culture Collection) and HeLa-Tat cells (AIDS Research and Reference Reagent Program, National Institutes of Health) were maintained in Dulbecco's modified Eagle's medium supplemented with 10% fetal bovine serum, 100 μg of streptomycin plus penicillin/ml, and 2 mM L-glutamine (Invitrogen).

Plasmids. To generate the $pMEp13^{II}$ plasmid, the coding sequence of $p13^{II}$ was amplified from pACH (22), an HTLV-1 infectious molecular clone, using the primers 5′ ATA CCT CGA GAT GCT TAT TAT CAG CCC A and 3′ TAT AGC GGC CGC TCG ATG CAA GC. The amplified product was cloned into the pBR322 (Stratagene, La Jolla, CA) shuttle vector. Concurrently, a 39-bp sequence of the influenza virus hemagglutinin (HA) epitope domain was amplified by oligonucleotide annealing using the primer pair 5′ AGC TTT ACC CAT ACG ATG TTC CAG ATT ACG CTA GCT TGC ATC GAT AAG 3′ and 5′ AAT TCT TAT CGA TGC AAG CTA GCG TAA TCT GGA ACA TCG TAT GGG TAA 3′ and was cloned into the 3′ end of the $p13^{II}$ sequence to tag the $p13^{II}$ protein with the HA epitope for immunodetection ($pBR322p13^{II}HA$). For the generation of the $pMEp13^{II}$ plasmid, the $p13^{II}HA$ segment was obtained from $pBR322p13^{II}HA$ by endonuclease digestion with XhoI and NotI and was then cloned into the pME18S plasmid (29; G. Franchini, National Cancer Institute, Bethesda, MD). The correct sequence was confirmed by Sanger DNA sequencing, and the expression of $p13^{II}HA$ was confirmed by anti-HA immunoblotting following transient transfection by electroporation in Jurkat cells.

For the construction of a transfer vector expressing $p13^{II}$ ($pWPTp13^{II}HA$), the $p13^{II}HA$-encoding fragment was obtained by restriction digestion and inserted into the pWPT-eGFP lentiviral transfer vector (D. Trono, University of Geneva, Geneva, Switzerland). The encephalomyocarditis virus internal ribosomal entry site element from the pHRCMV-Tax-eGFP plasmid (39) was obtained by PCR amplification and cloned downstream of $p13^{II}HA$ for the translation of a bicistronic enhanced green fluorescent protein (eGFP)- and $p13^{II}$-expressing mRNA. The pWPT transfer vector with $p13^{II}HA$ inserted in a reverse orientation (pWPT) was also made and used as a mock control vector.

Production of vesicular stomatitis virus glycoprotein-pseudotyped $p13^{II}$ lentiviral expression vector. To stably express $p13^{II}$, a lentiviral vector was generated using a packaging plasmid (pCMVΔ8.2) and a vesicular stomatitis virus glycoprotein plasmid (pHCMV-G) for packaging. The vector was produced by transient transfection of three plasmids (pCMVΔ8.2, pHCMV-G, and pWPT transfer vectors) into 293T packaging. In brief, 1.2×10^7 early-passage 293T cells were seeded into 0.01% poly-L-lysine (Sigma, St. Louis, MO)-coated 15-cm culture dishes on the day before transfection. The cells were transfected with 5 μg of pCMV-G, 25 μg of pHCMVΔR8.2, and 25 μg of either pWPT- $p13^{II}HA$ or pWPT by calcium phosphate-mediated transfection. The culture supernatants were collected at 24-h intervals for 96 h, cleared of cellular debris by centrifugation at $500 \times g$ for 10 min, and filter sterilized (0.2 μm). The filtered supernatants were concentrated by centrifugation ($6,000 \times g$ for 16 h at 4°C). The pellet was suspended in 300 μl of complete Dulbecco's modified Eagle's medium overnight at 4°C, and the concentrated virus was stored at −80°C.

To determine the virus titer, virus stocks diluted 1:100, 1:1,000, or 1:10,000 were used to infect 293T cells, and eGFP expression was measured by flow cytometry at 48 h postinfection as described previously (15). Briefly, on the day before infection, 1×10^5 293T cells were seeded into a six-well plate. The medium was removed the following day, and the cells were then incubated with diluted virus-containing medium with Polybrene (5 μg/ml) (Sigma). The cells were spin infected by centrifugation at $1,400 \times g$ for 1 h at 32°C and then left in the virus-containing medium for 16 h. After being fed with fresh medium and cultured for 48 h, the cells were collected and analyzed by fluorescence-activated cell sorting (FACS) using an ELITE ESP flow cytometer (Beckman Coulter, Fullerton, CA).

Lentiviral infection. Jurkat T cells (2.5×10^6 cells in 2 ml), 293T cells, or HeLa-Tat cells (both at 1×10^6 cells in 2 ml) were spin infected ($1,400 \times g$ at 32°C for 1 h) with the $pWPTp13^{II}HA$ or pWPT mock lentiviral vector at a multiplicity of infection of 5 in the presence of Polybrene at 5 μg/ml (Sigma). The cells were left in the virus-containing medium for 16 h, fed with fresh medium, and cultured for at least 4 days to analyze $p13^{II}$ expression by Western immunoblotting.

DNA plasmid transfection. Jurkat T cells (1×10^7) were electroporated with 5, 10, or 20 μg of $pMEp13^{II}$ plasmid, using a Nucleofector kit (Amaxa Biosystems, Gaithersburg, MD) according to the manufacturer's instructions. The total amount of plasmid transfected into each sample was adjusted to 20 μg with pME18S (pME) plasmid. For Ras transfection, 1×10^7 Jurkat T cells were transfected with 20 μg of an Ha-Ras expression vector (pCMV-Ha-Ras) (BD Biosciences, San Jose, CA), using a Nucleofector kit (Amaxa Biosystems) according to the manufacturer's instructions. At 48 h posttransfection, the cells were collected and treated as described below.

Immunoprecipitation and Western blot assays. The expression of $p13^{II}$ was analyzed by Western blot assays. In brief, lentiviral vector-infected or transiently transfected cells were lysed in radioimmunoprecipitation assay (RIPA) buffer (150 mM NaCl, 50 mM Tris [pH 8.0], 10 mM EDTA, 10 mM NaF, 10 mM $Na_4P_2O_7 \cdot H_2O$, 1% NP-40, 0.5% deoxycholic acid, 0.1% sodium dodecyl sulfate [SDS], 1 mM sodium orthovanadate, 1 mM phenylmethylsulfonyl fluoride, and Complete protease inhibitor [Roche Applied Science, Indianapolis, IN]), and the cell lysates were cleared by centrifugation (4°C at $16,000 \times g$ for 15 min). Protein concentrations were determined with a BCA assay (micro-BCA protein assay; Pierce, IL), and a total of 50 μg of 293T cell lysates or 300 μg of infected Jurkat T-cell lysates was separated by SDS-15% polyacrylamide gel electrophoresis, followed by transfer to nitrocellulose membranes. Membranes were blocked with 5% nonfat dry milk in phosphate-buffered saline (PBS) with 0.1% Tween overnight, incubated with a mouse anti-HA monoclonal antibody (Ab; 1:1,000) (clone 16B-12; Covance Research Products, Princeton, NJ) overnight at 4°C, and developed by using a horseradish peroxidase-labeled secondary Ab (1:1,000) and an enhanced chemiluminescence reagent (Cell Signaling Technology, Beverly, MA).

For the detection of Ras, whole-cell lysates were prepared as described above. Five hundred micrograms of cell lysates were incubated with a 1:150 dilution of a mouse monoclonal anti-Ras Ab (Oncogene Research Products, San Diego, CA) overnight at 4°C. The immune complex mixture was then incubated with 50 μl of protein A/G plus agarose beads (Santa Cruz Biotechnology, Santa Cruz, CA) for 3 h. The beads were washed five times in RIPA buffer and boiled in SDS sample buffer, and supernatants were analyzed by Western immunoblotting using a mouse anti-Ras monoclonal Ab (1:1,000).

Cell growth and viability loss assays. For comparisons of cell growth curves, 1×10^5 to 5×10^5 viable Jurkat T cells were seeded into 24-well culture plate with 1 ml fresh medium. Viable cell numbers were counted by trypan blue dye exclusion every 24 h for 5 days. For additional cell growth and viability loss assays, an MTS [3-(4,5-dimethylthiazol-2-yl)-5-(3-carboxymethoxyphenyl)-2-(4-sulfophenyl)-2H-tetrazolium, inner salt] colorimetric cell viability assay kit (Promega, Madison, WI) was used according to the manufacturer's instructions. For stimulation protocols, Jurkat T cells were incubated with medium containing 20 ng/ml phorbol 12-myristate 13-acetate (PMA; Sigma)/ml, 2 μM ionomycin (Sigma), or a combination of 10 U/ml human interleukin-2 (Roche Applied Science) and 2 μg/ml phytohemagglutinin (Sigma). For stimulation with CD3/CD28 antibodies, 1 μg each of a mouse anti-human CD3 monoclonal antibody (clone HIT3a) and a mouse anti-human CD28 monoclonal antibody (clone Cd28.2; BD Pharmingen, San Diego, CA) was immobilized on an enzyme immunoassay-radioimmunoassay plate (Costar, Chicago, IL) in binding buffer (0.2 M sodium bicarbonate [pH 8.0]) overnight at 4°C. The wells were washed three times with PBS, followed by the addition of cells. At the end of the

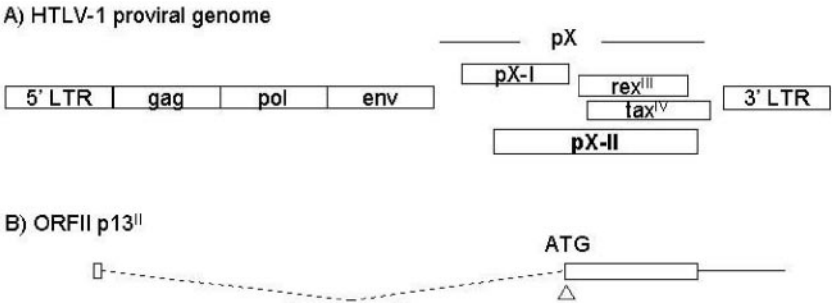

FIG. 1. HTLV-1 provirus genome and p13^{II} coding region. (A) Schematic representation of HTLV-1 provirus genome indicating four distinct open reading frames (ORFs) in the pX region (pX-I through -IV) represented by open boxes. The viral proteins p12^{I}, p13^{II} and p30^{II}, Rex^{III}, and Tax^{IV} are encoded by pX-I through -IV, respectively. (B) Schematic representation of p13^{II} transcript (box). p13^{II} is a product of a singly spliced mRNA from ORFII (pX-II). The location of the start codon is shown (arrowhead).

incubation, 20 μl of MTS reagent was added to each well and incubated for an additional 60 min. A photospectrometric microplate reader (Beckman Coulter, Fullerton, CA) was used to measure the optical density at 490 nm. For MTS cell viability loss assays, 40,000 viable cells were seeded in 96-well plates with various concentrations of FasL (0.2 to 0.8 μg/ml; Biomol, Plymouth Meeting, PA) or C2-ceramide (30 μM to 120 μM; Biomol) in a total volume of 100 μl per well for 6 h. All MTS experiments were performed with three or four replicates, and a minimum of two independent experiments were performed.

Annexin V apoptosis assay. Viable Jurkat T cells (2×10^5) were seeded into 24-well plates with fresh medium containing FasL (0.2 to 0.8 μg/ml; Biomol) or C2-ceramide (20 μM to 120 μM; Biomol) in a total volume of 1.0 ml per well for 1 to 4 h. zVAD.fmk and zIETD.fmk are inhibitors of pan-caspase and caspase 8, respectively (Biomol). Where indicated, the cells were preincubated with 20 μM of either zVAD.fmk or zIETD.fmk for 4 h prior to exposure to FasL (see Fig. 4A). The annexin V apoptosis assay was performed using an annexin V Alexa Fluor 647 conjugate (Molecular Probes, Eugene, OR) according to the manufacturer's instructions. In brief, the cells were collected, washed once with PBS, and resuspended in 100 μl of annexin-binding buffer (10 mM HEPES, 140 mM NaCl, and 2.5 mM $CaCl_2$, pH 7.4), followed by incubation with 5 μl of annexin V conjugate solution and 5 μl of 30 μM propidium iodide (PI) for 15 min at room temperature. After the incubation period, 400 μl of the annexin-binding buffer was added and mixed gently, and the samples were kept on ice. The samples were analyzed by flow cytometry (FACS Calibur; BD Coulter), and the data were analyzed using ProQuest software (BD Biosciences). For each sample, 10,000 gated cells were examined for their annexin V and PI staining, and the percentage of cells in early apoptosis was defined by measuring the high-annexin V- and low-PI-staining cell population, represented in the lower right quadrant of FACS analysis data (see Fig. 4A). All annexin V assays were performed in triplicate, and a minimum of two independent experiments were performed. Statistical analysis was performed by using Student's *t* tests. *P* values of <0.05 were considered significant.

Chemical blocking of Ras-mediated apoptosis. B581 (Biomol) is a farnesyl transferase inhibitor (FTI). Where indicated, Jurkat T cells were incubated with cRPMI containing either 50 or 200 nM of B581 for 16 h prior to exposure to FasL. To assess the potential toxicity of B581, the cells were also treated with 200 nM of B581 alone without a subsequent exposure to ceramide or FasL. Annexin V apoptosis assays were then performed as described above.

Immunofluorescence staining and confocal microscopy. To verify the mitochondrial localization of p13^{II}, HeLa-Tat cells that were spin infected with the lentiviral vector at a multiplicity of infection of 5 were seeded into LAB-TEK chamber slides (Nalgene Nunc International, Rochester, NY). The cells were then fixed for 15 min in 4% paraformaldehyde at 24 h after being seeded, followed by permeabilization with 0.2% Triton X-100 (Sigma) for 5 min. Nonspecific binding sites were blocked with PBS containing 1% bovine serum albumin for 1 h at 37°C. After three washes, cells were incubated with mouse anti-human cytochrome *c* oxidase complex IV immunoglobulin G2a (IgG2a; 1:100) (Molecular Probes) as a mitochondrion-specific marker and with a secondary goat anti-mouse IgG2a Alexa Fluor 647 conjugate (1:200) (Molecular Probes) for 1 h each at room temperature. The p13^{II} protein was stained with mouse anti-HA IgG1 (clone 16B-12; Covance Research Products) after preincubation with anti-mouse IgG1-Fc $F(ab)_2$ Zenon anti-HA (Molecular Probe) for 1 h at room temperature. HeLa-Tat cells that were spin infected with mock viral vector were used as a negative control.

For analyses of Ras expression and subcellular localization, HeLa-Tat cells stably infected with p13^{II}-expressing or mock control lentiviral vector were prepared as described above. Cell nuclei were stained with bisbenzimide H33528 (Hoechst 33528; Calbiochem, San Diego, CA) for 30 min at 37°C. The cells were fixed and blocked as described above and were then incubated with a mouse anti-pan-Ras antibody (1:150; Oncogene Research) and a secondary rabbit anti-mouse IgG-Alexa Fluor 546 conjugate (1:200) (Molecular Probes) for 1 h each at room temperature. A mouse IgG1 antibody (Caltag Laboratories, Burlingame, CA) was used as an isotype control. Fluorescence confocal microscopy and image collection were performed using a Leica TCS SP2 fluorescence microscope system, and images were analyzed with LCS software (Leica Microsystems, Bannockburn, IL).

RESULTS

Expression of HTLV-1 p13^{II} in Jurkat T lymphocytes. A stable expression system for p13^{II} in Jurkat T cells using a lentiviral vector system was established to test the influence of the HTLV-1 mitochondrion-localizing protein p13^{II} on T-lymphocyte responses to apoptotic stimuli (Fig. 1). Corresponding mock cell lines were generated by spin infecting Jurkat T cells with a mock lentiviral vector. The stable expression of p13^{II} was verified by a Western immunoblot assay (Fig. 2A). Specific mitochondrial localization and a mitochondrial targeting motif for p13^{II} have been reported (5). Our HA epitope-tagged p13^{II} expressed using the lentiviral vector system also colocalized with the cytochrome *c* dehydrogenase complex protein, a mitochondrion-specific marker, in HeLa-Tat cells (Fig. 2B).

Both direct cell counting and MTS colorimetric assays were performed to examine Jurkat T cells for possible changes in cell viability and growth pattern under normal culture conditions associated with the stable expression of p13^{II}. Cultures with a low seeding density (5×10^4 to 10×10^4 cells/ml) did not reveal a significant difference in cell proliferation between two pairs of independently established p13^{II}-expressing cell lines and their corresponding mock lines (data not shown). We then examined cell growth starting with a higher seeding density (5×10^5 cells/ml) (Fig. 3A). At later time points, the p13^{II}-expressing line showed reduced proliferation compared to the mock line. The data indicated that the lentiviral vector-mediated constitutive expression of p13^{II} did not alter the growth pattern of Jurkat T cells under normal culture conditions but resulted in reduced proliferation associated with a high-cell-density environment.

Next, we examined the proliferation responses of Jurkat T

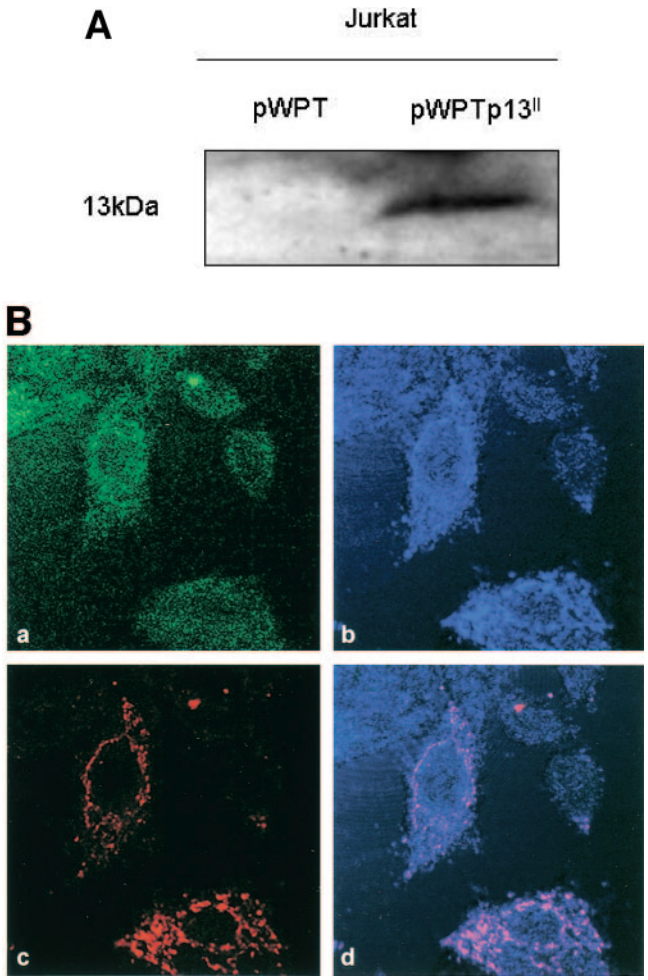

FIG. 2. Expression and mitochondrial localization of $p13^{II}$. (A) Stable expression of HA epitope-tagged $p13^{II}$ in Jurkat cells, demonstrated by a Western immunoblot assay. Jurkat T cells were infected with a $p13^{II}$-expressing (pWPTp13^{II}) or mock (pWPT) lentiviral vector at a multiplicity of infection of 5. The cell lysates were subjected to SDS-polyacrylamide gel electrophoresis, followed by immunoblotting using a mouse monoclonal anti-HA antibody. (B) Mitochondrial localization of $p13^{II}$. HeLa-Tat cells were infected with the $p13^{II}$-expressing lentiviral vector at multiplicity of infection of 5. The cells were then stained for an immunofluorescence analysis of $p13^{II}$ expression and colocalization with mitochondria. (a) eGFP; (b) cytochrome *c* oxidase complex IV; (c) $p13^{II}$; (d) overlay image. Mock viral vector-infected cells were used as negative controls (not shown).

cells, with or without stable $p13^{II}$ expression, in the presence of various known growth stimulants, using MTS colorimetric assays. The cells were incubated with media containing ionomycin, phorbol myristate acetate, combinations of human IL-2 and phytohemagglutinin, or anti-CD3 and anti-CD28 antibodies in order to elicit proliferation as previously described (1). Our data indicated no significant difference in response to any combination tested between the $p13^{II}$-expressing and mock cell lines (Fig. 3B) compared by average increases in optical density over the values for unstimulated samples of the corresponding parental cell lines. A series of proliferation assays performed under these conditions and measured by using tritiated thymidine revealed the same results (data not shown).

To further investigate potential phenotypic changes in Jurkat T cells due to stable $p13^{II}$ expression, the cells were analyzed for the magnitude of viability loss upon treatment with ceramide and FasL, known inducers of apoptotic cell death in lymphocytes. Compared to the untreated cells, the $p13^{II}$-expressing Jurkat T cells exhibited a significant loss of viability ($P < 0.05$) at concentrations above 0.4 μg/ml and 30 μM for FasL and ceramide, respectively (Fig. 3C), indicating a significant magnitude of apoptotic events in $p13^{II}$-expressing Jurkat T cells induced by these agents.

$p13^{II}$-expressing lymphocytes are sensitive to apoptosis induced by FasL and ceramide. Based on the observation that the $p13^{II}$-expressing Jurkat cells resulted in a pronounced viability loss upon stimulation with known inducers of lymphocyte apoptosis, we then performed apoptosis-specific annexin V assays to further characterize the differences in apoptosis responses among these cells. FasL treatment of $p13^{II}$-expressing Jurkat T cells resulted in a marked induction of an early apoptotic cell population (42.0% for the FasL-treated versus 4.6% for the untreated cell population) (Fig. 4A, top panels). The specificity of the assay was verified by preincubation of the cells with zVAD.fmk (a pan-caspase inhibitor) or zIETD.fmk (a caspase 8 inhibitor) prior to treatment with FasL. Both inhibitors resulted in a nearly complete block of annexin V staining (4.2% and 3.5%, respectively) upon exposure to an apoptosis-inducing concentration (0.4 μg/ml) of FasL (Fig. 4A, bottom panels).

A comparison of the degrees to which apoptosis was induced by FasL was made by annexin V assays performed on two independently established Jurkat T-cell lines (p13-1 and p13-2) stably expressing $p13^{II}$ and on their corresponding mock control lines (Mock-1 and Mock-2) (Fig. 4B). The results showed that the $p13^{II}$-expressing Jurkat T cells underwent significantly more apoptosis at all doses of FasL tested ($P < 0.001$). For each experiment, the constitutive expression of $p13^{II}$ in p13-1 and -2 and comparable levels of surface Fas expression were verified by Western immunoblot assays (data not shown). To answer the question of whether the sensitization to apoptosis was dependent on the amount of $p13^{II}$ expressed in Jurkat T cells, we performed transient transfection assays with the $p13^{II}$ expression plasmid (pMEp13^{II}), followed by exposure of the cells to fixed, apoptosis-inducing concentrations of FasL (0.4 μg/ml) and ceramide (60 μM) (Fig. 5A and B). Although the increasing level of $p13^{II}$ expression itself did not induce apoptosis, subsequent exposures to both FasL and ceramide were associated with increased sensitivities to apoptosis (18.3 ± 2.9% and 4.9 ± 0.19% early apoptotic cells in Jurkat T cells without $p13^{II}$ versus 38.19 ± 0.56% and 26.11 ± 0.4% in cells transfected with 20 μg of pMEp13^{II} plasmid, upon FasL and ceramide exposure, respectively).

FasL-induced apoptosis was reduced by pretreatment of $p13^{II}$-expressing cells with a chemical inhibitor of Ras. We then sought to explore possible molecular pathways that predisposed the $p13^{II}$-expressing cells to apoptosis. Both FasL and ceramide play a critical role in the regulation of apoptosis in Jurkat T cells, and Fas-FasL engagement results in a caspase 8-mediated activation of endogenous acidic sphingomyelinase, a potent inducer of ceramide accumulation during lymphocyte apoptosis (19, 34). Ras-mediated signaling is a key regulator of both FasL- and ceramide-induced apoptosis in lymphocytes

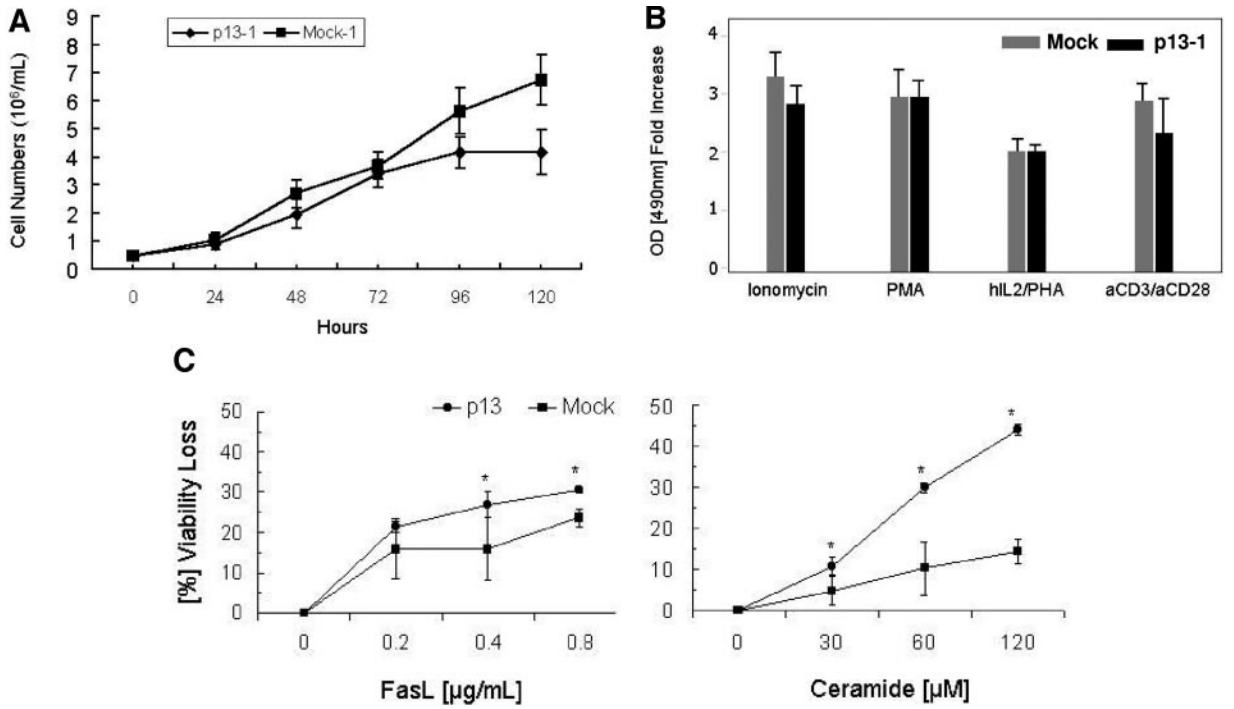

FIG. 3. Expression of p13^{II} in Jurkat T cells suppresses cell proliferation at a high seeding density and results in a more pronounced viability loss upon exposure to FasL and ceramide. (A) Proliferation of lentiviral vector-infected Jurkat T cell lines with (p13-1) or without (Mock-1) p13^{II}, examined by direct counting. The data show average values of quadruplicate samples ± standard deviations. Representative results of two independent experiments are shown. (B) Lentiviral vector-infected Jurkat cell lines with (p13-1) or without (mock) p13^{II} were compared for their proliferation responses to common stimuli of lymphocytes in an MTS assay. Each bar represents the average fold increase in optical density compared to the corresponding unstimulated cell line with the standard deviation of triplicate samples. (C) Viability loss assay. Lentiviral vector-infected Jurkat cell lines with (p13) or without (mock) p13^{II} were analyzed for a loss of viability upon exposure to FasL (left) and ceramide (right). Each point represents the average of triplicates, showing the loss of viability measured as the % loss in optical density compared to the corresponding untreated cell line, with the standard deviation indicated with error bars. Representative results of two independent experiments are shown. *, $P < 0.05$ by Student's t test.

(18), which can be altered using farnesyl transferase inhibitors (FTIs), which affect the posttranslational prenylation of Ras (7, 20, 35, 38).

To verify that an increased amount of Ras can sensitize Jurkat T cells to FasL-induced apoptosis and to test the specificity of FTI as an inhibitor of Ras function, we performed a transfection experiment where the Jurkat T cells were transiently transfected with a plasmid expressing wild-type Ha-Ras and subsequently exposed to apoptosis-inducing concentrations of FasL (Fig. 6A). The results showed that a transient overexpression of wild-type Ha-Ras was associated with an increased magnitude of apoptosis upon exposure to a fixed concentration of FasL (0.4 μg/ml), whereas the expression of Ha-Ras itself did not induce apoptosis (Fig. 6A, fourth bar). Secondly, the cells were pretreated with commercially available FTI posttransfection for 16 h prior to exposure to FasL to test its effectiveness at inhibiting Ras-mediated function (e.g., apoptosis). Our results showed a significant reduction in the magnitude of apoptosis in the cells overexpressing Ha-Ras, even upon exposure to FasL (Fig. 6A, last bar).

Subsequently, the pretreatment of the p13^{II}-expressing Jurkat T cells with FTI was followed by FasL exposure, and alterations in apoptotic responses were measured by an annexin V assay. Our results indicated significant reductions of apoptosis in FTI-pretreated Jurkat T cells (Fig. 6B). The percentage of cells undergoing early apoptosis upon FasL exposure was reduced from 51.54 ± 0.57% without FTI treatment to 32.52 ± 2.76% in cells pretreated for 16 h with 50 nM of FTI prior to exposure to FasL. The increased concentration of FTI resulted in a reduction in apoptosis, as the percentage of early apoptotic cells was further reduced to 8.75 ± 1.20% when pretreated with a higher concentration of FTI (200 nM). These results indicated that Ras is a principal modulator of apoptosis in p13^{II}-expressing Jurkat T cells. Western blot assays were performed to verify that the expression of p13^{II} in the FTI-treated cells was unaffected (data not shown).

Subcellular localization of Ras is not altered by p13^{II} expression. We then examined Jurkat T cells with or without p13^{II} to determine whether the increased sensitivity of p13^{II}-expressing cells to FasL- and ceramide-induced apoptosis was due to increased amounts of or alterations in the subcellular localization of Ras. Immunoprecipitation of Ras in the cellular lysates under normal culture conditions followed by Western immunoblotting revealed no apparent difference in the total amount of Ras between p13^{II}-expressing and corresponding mock cell lines (Fig. 7A). There were also no observable differences in the subcellular localization of Ras in p13^{II}-expressing and mock-infected HeLa-Tat cells (Fig. 7B). Furthermore, Ras did not appear to be colocalized with p13^{II} in mitochondria in HeLa-Tat cells (data not shown).

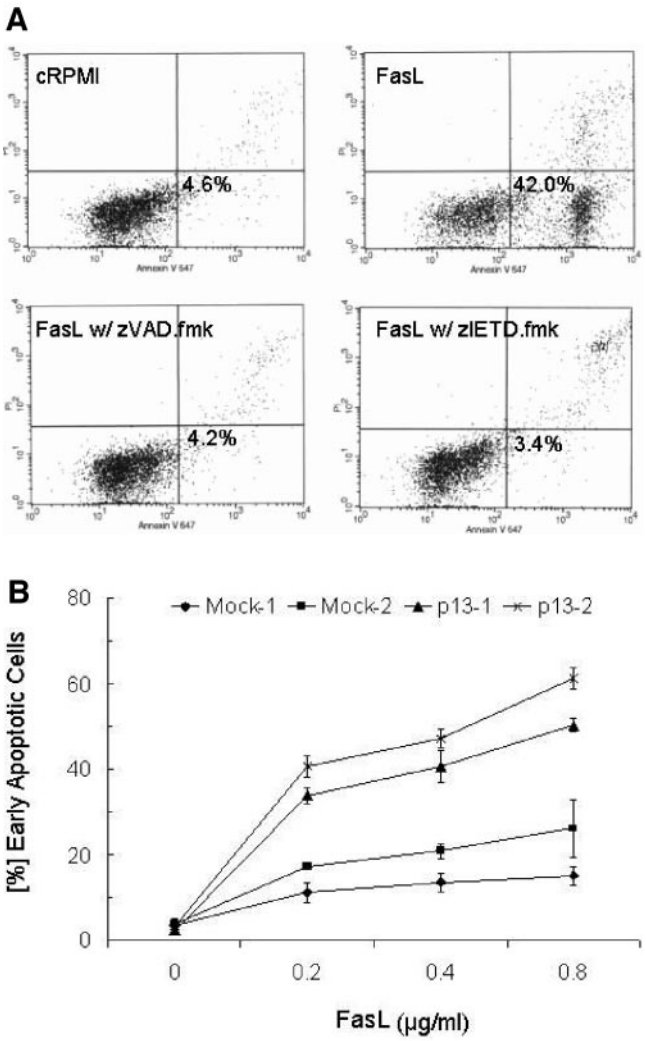

FIG. 4. $p13^{II}$ sensitizes Jurkat T cells to FasL-induced apoptosis. (A) Flow cytometric analysis of Jurkat T cells demonstrating increased sensitivity of $p13^{II}$-expressing cells to apoptosis induced by FasL. A representative result of the annexin V apoptosis assay is shown. The marked induction of apoptosis by exposure to FasL is shown as a shift of the cell population into the lower right quadrant by FACS analysis. cRPMI, normal growth medium; FasL, cRPMI supplemented with 0.4 μg/ml FasL; zVAD.fmk, pan-caspase inhibitor; zIETD.fmk, caspase 8 inhibitor. The boxed numbers indicate the percentages of the total cell population analyzed that were in early apoptotic phase, defined as high-annexin-V- and low-propidium-iodide-staining cells appearing in the lower right quadrant. (B) Graph indicating average values (% early apoptotic cells) of three independent experiments using two independently generated lentiviral vector-infected Jurkat T-cell lines, either with (pWPT-$p13^{II}$; p13-1 and -2) or without (pWPT; Mock-1 and -2) $p13^{II}$. Error bars represent the corresponding standard deviations.

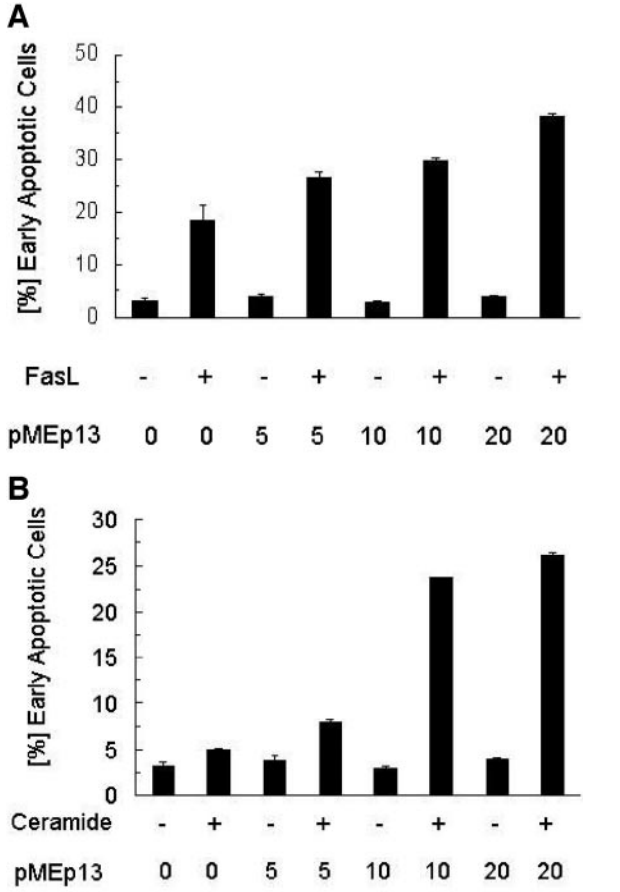

FIG. 5. Sensitization of Jurkat T cells to apoptosis is $p13^{II}$ dose dependent. Transient transfections of $p13^{II}$ and annexin V apoptosis assays were performed. Increasing amounts (0, 5, 10, and 20 μg per 1×10^7 cells) of $pMEp13^{II}$ plasmid were transfected into Jurkat T cells. Forty-eight hours after each transfection, the cells were exposed to either 0.4 μg/ml FasL (A) or 60 μM ceramide (B) for 4 h, followed by annexin V apoptosis assays. Each bar represents the average percentage of the cells in early apoptosis, with the error bar showing the standard deviation for triplicate wells. The increasing expression levels of $p13^{II}$ were verified by anti-$p13^{II}$HA Western immunoblotting (data not shown).

DISCUSSION

The HTLV-1 accessory protein $p13^{II}$ selectively localizes to the inner membranes of mitochondria and also interacts with farnesyl pyrophosphate synthetase, which catalyzes the synthesis of farnesyl pyrophosphate, an essential substrate of Ras posttranslational modifications (5, 8, 24, 25). In this study, we analyzed the ability of HTLV-1 $p13^{II}$ to alter the response of Jurkat T lymphocytes to apoptosis-inducing stimuli. Our data revealed that stable and transient $p13^{II}$ expression in Jurkat T cells was associated with an increased sensitivity to apoptosis induced by both ceramide and FasL, in a dose-responsive manner. We demonstrated that this activity was caspase dependent, using inhibitors of pan-caspases and caspase 8. Furthermore, sensitization of the cells to apoptosis by $p13^{II}$ was reduced by pretreatment of the cells with B581, a farnesyl transferase inhibitor (FTI) which blocks the posttranslational prenylation of Ras. We extended this observation by correlating the overexpression of Ras with an increased sensitivity to FasL-induced apoptosis in Jurkat T cells. Collectively, our data reveal that $p13^{II}$, a mitochondrion-localizing protein of HTLV-1, alters the lymphocyte response to apoptotic stimuli in a Ras-mediated manner.

Ras-mediated signaling plays many roles in cell survival, proliferation, transformation, and the modulation of apoptosis (7, 26). The regulation of apoptosis by Ras depends on many factors, including the isoform, subcellular localization, and

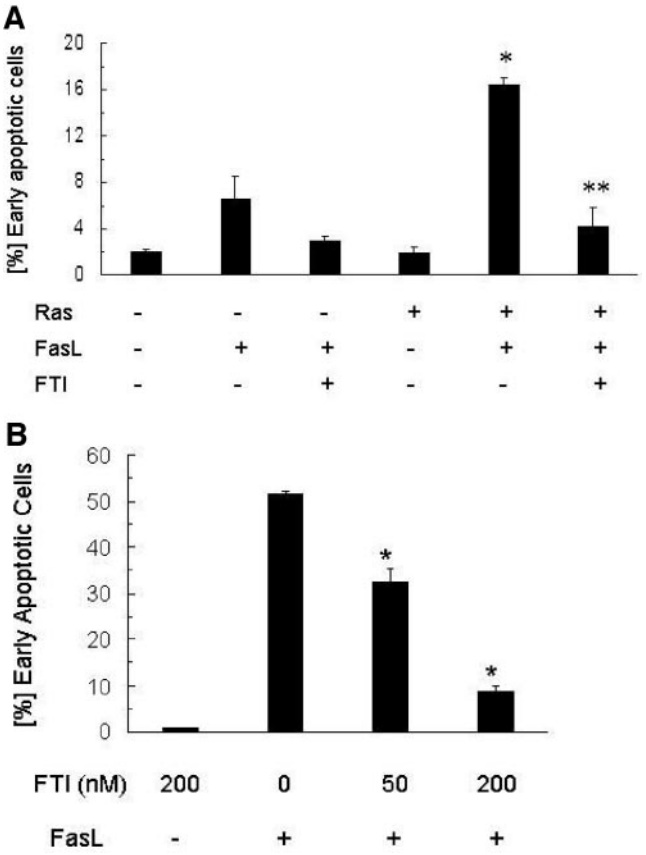

FIG. 6. Overexpression of Ha-Ras sensitizes Jurkat T cells to FasL-induced apoptosis, and FTI blocks FasL-induced, Ras-mediated apoptosis. (A) Jurkat T cells were transiently transfected with wild-type Ha-Ras expression plasmids (right three bars), and their early apoptosis responses were compared to those induced by FasL exposure. The overexpression of Ras sensitized Jurkat T cells to FasL-induced apoptosis (*, significant difference between second and fifth bars [$P < 0.01$]). Pretreatment of the cells with FTI for 16 h prior to FasL exposure resulted in a significant reduction of apoptosis (**, significant difference between fifth and sixth bars [$P < 0.01$]). Each bar represents the average percentage of cells in early apoptosis from three independent samples ± the standard deviation. (B) Graph demonstrating that p13^{II}-sensitized, FasL-induced apoptosis in Jurkat T cells is mediated by Ras. p13^{II}-expressing Jurkat T cells were incubated with FTI for 16 h prior to exposure to FasL (0.4 μg/ml for 4 h). The sensitivity to apoptosis in p13^{II}-expressing Jurkat cells could be significantly reduced by increasing the dose of FTI, a down-regulator of Ras protein. The results shown are the average percentages of cells in early apoptosis from triplicate wells for each treatment ± standard deviations, measured by an annexin V apoptosis assay (*, $P < 0.001$ by Student's t test).

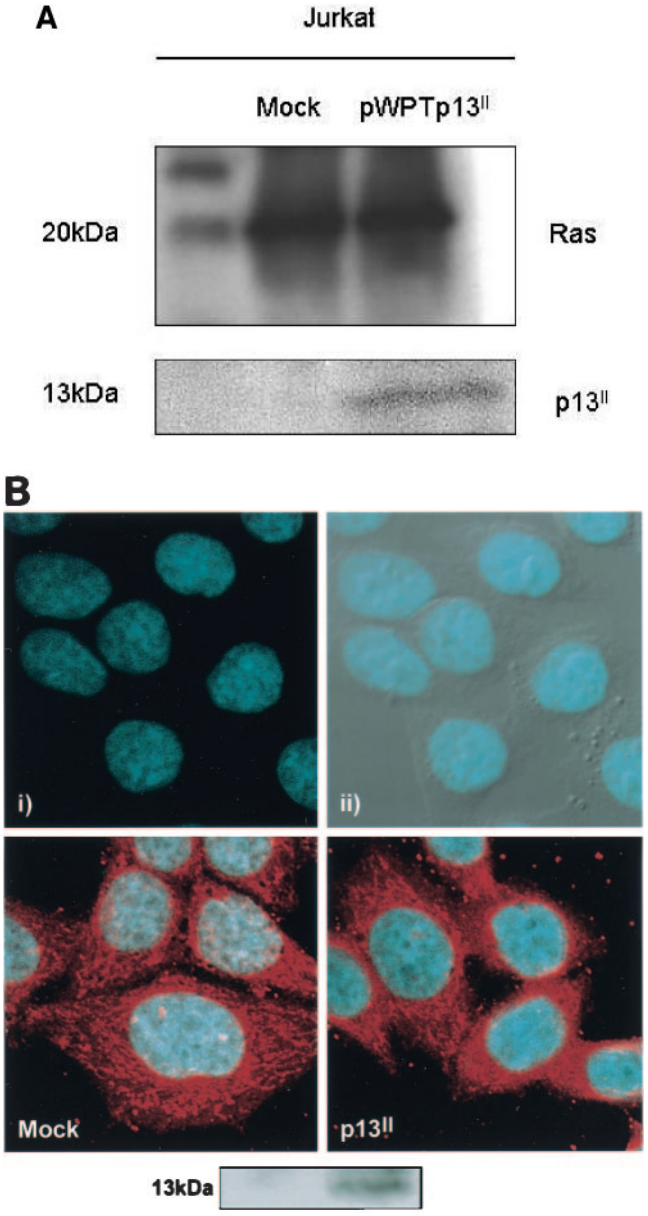

FIG. 7. Cellular Ras level and localization were not altered by p13^{II} expression. (A) Ras immunoprecipitation and Western blotting. Cell lysates from p13^{II}-expressing (pWPT p13^{II}) and mock (pWPT) Jurkat T-cell lines were subjected to immunoprecipitation and Western immunoblotting for a comparison of the amounts of 21-kDa Ras protein under normal culture conditions. The constitutive expression of p13^{II} in the pWPT-carrying p13^{II} cell line was verified by anti-p13HA Western immunoblotting (bottom). (B) Cellular localization of Ras is not affected by p13^{II} expression. The immunofluorescence confocal microscopic images show that the levels of Ras and its cytoplasmic localization are not altered by p13^{II} (mock versus p13^{II}). (i) Isotype staining control with nonspecific mouse IgG antibody. (ii) Phase-contrast overlay on image i. The expression of p13^{II} was verified by anti-p13^{II}HA Western immunoblotting (bottom inset). Original magnification, ×630 for all panels.

posttranslational modification of the signaling protein (7). The detailed mechanisms by which Ras mediates apoptosis remain unclear, but they appear to involve the dysregulation of proteins downstream of Ras signaling, including transcription factors (6). In addition, unique isoforms of Ras appear to traffic to mitochondria upon FasL stimulation and directly bind Bcl-2, counteracting Bcl-2's antiapoptotic function in Jurkat T lymphocytes (13). A number of viral proteins that localize to mitochondria play roles in the regulation of apoptosis (10). Our data are the first to suggest that p13^{II} in HTLV-1-infected cells serves to modify the functional response of mitochondria to Ras-mediated signaling that controls cell survival. Interestingly, *Bovine leukemia virus*, another member of the *Deltaretrovirus* genus, encodes an analogous accessory protein, G4, which also localizes to mitochondria, and both p13^{II} and G4 directly interact with farnesyl pyrophosphate synthetase (25).

These observations suggest a role for these proteins in the function of farnesyl pyrophosphate, an essential substrate of Ras posttranslational modifications. In this regard, it is interesting that bovine leukemia virus G4 was reported to require the cotransfection of Ras to enhance the tumorigenicity of transplanted rat embryonal fibroblasts in mice (21). In addition, we have recently reported that the expression of $p13^{II}$ in HeLa cells was associated with a significant suppression of the tumorigenicity of c-Myc- and Ha-Ras-cotransfected rat embryonal fibroblasts in a nude mouse model, providing additional evidence for the involvement of Ras in $p13^{II}$-associated alterations in cell functions (36). Consistent with our previous report (36), the $p13^{II}$-expressing Jurkat T-cell lines used for the present study also exhibited reduced proliferation at a high seeding density compared to mock vector cell lines. It is likely that $p13^{II}$-expressing cells are reactive to cellular stress (e.g., reduced growth factors) associated with high-density culture conditions in a similar manner to their reactivity to apoptotic signals. Our findings reported herein further support the role of this accessory protein in modifying mitochondrion-mediated responses of lymphocytes to signaling events involving cell survival.

Our data provide intriguing evidence of a link between the Ras pathway and the HTLV-1 viral protein $p13^{II}$ in human lymphocytes. It seems that $p13^{II}$ does not alter the constitutive level of cellular Ras in Jurkat T cells or its subcellular localization in HeLa-Tat cells under normal culture conditions. We found that Ras does not appear to be colocalized with $p13^{II}$ in HeLa-Tat cells by fluorescence confocal microscopy (data not shown). The biological significance of the potential association of $p13^{II}$ with the Ras pathway, particularly in the context of HTLV-1 infection in human lymphocytes, remains to be determined. Unfortunately, there are no published reports that directly address the expression of this unique viral accessory protein during infection in HTLV-1-infected subjects or patients with disease. We therefore are unable to compare the levels of $p13^{II}$ expression achieved in the present study with those in lymphocytes during natural HTLV-1 infections. Determining the amount of any HTLV-1 protein in vivo has been difficult to do, in part because of the highly cell-associated manner of transmission of the virus in vivo. For our study, we designed $p13^{II}$ expression to be under the influence of the hematopoietic EF1α cellular promoter. This expression system resulted in low and stable constitutive expression of $p13^{II}$ to mimic the low expression level in lymphocytes. The $p13^{II}$-mediated modulation of apoptotic stimuli in HTLV-1-infected cells may represent a mechanism by which the virus modifies the survival of a subset of infected cells (e.g., high-virus-expressing cells) to avoid the host immune system. To test the influence of $p13^{II}$ in the context of HTLV-1 infection, our present studies have focused on an HTLV-1 infectious molecular clone that lacks the ability to express $p13^{II}$. The data presented herein are the first to indicate that HTLV-1 $p13^{II}$ alters the balance in Ras-mediated lymphocyte survival, and they provide new insights into HTLV-1-induced lymphocyte proliferation. These findings illustrate that further studies are needed to compare the complementary or competing roles of HTLV-1 regulatory (Tax and Rex) and accessory (e.g., $p13^{II}$) proteins in HTLV-1 replication and associated disease. Additionally, future analyses focusing on the Ras-mediated function in lymphocytes will be of great interest and will provide a further understanding of the mechanisms by which HTLV-1 regulates the survival of infected lymphocytes.

ACKNOWLEDGMENTS

We thank G. Franchini and D. Trono for providing the plasmids, M. Kotour for technical support with confocal microscopy, B. Regner for flow cytometric analysis, and S. Fernandez for statistical consultation.

This work was supported by grants P01 CA100730 and R01 RR14324 (M.L.) from the National Cancer Institute and R03 TW05705 (M.L. and V.C.) from Fogarty Foundation, National Institutes of Health.

REFERENCES

1. **Albrecht, B., and M. D. Lairmore.** 2002. Critical role of human T-lymphotropic virus type 1 accessory proteins in viral replication and pathogenesis. Microbiol. Mol. Biol. Rev. **66:**396–406.
2. **Bartoe, J. T., B. Albrecht, N. D. Collins, M. D. Robek, L. Ratner, P. L. Green, and M. D. Lairmore.** 2000. Functional role of pX open reading frame II of human T-lymphotropic virus type 1 in maintenance of viral loads in vivo. J. Virol. **74:**1094–1100.
3. **Ciminale, V., D. D'Agostino, L. Zotti, G. Franchini, B. K. Felber, and L. Chieco-Bianchi.** 1995. Expression and characterization of proteins produced by mRNAs spliced into the X region of the human T-cell leukemia/lymphotropic virus type II. Virology **209:**445–456.
4. **Ciminale, V., G. N. Pavlakis, D. Derse, C. P. Cunningham, and B. K. Felber.** 1992. Complex splicing in the human T-cell leukemia virus (HTLV) family of retroviruses: novel mRNAs and proteins produced by HTLV type I. J. Virol. **66:**1737–1745.
5. **Ciminale, V., L. Zotti, D. M. Dagostino, T. Ferro, L. Casareto, G. Franchini, P. Bernardi, and L. Chiecobianchi.** 1999. Mitochondrial targeting of the p13(II) protein coded by the x-II ORF of human T-cell leukemia/lymphotropic virus type I (HTLV-I). Oncogene **18:**4505–4514.
6. **Cox, A. D., and C. J. Der.** 2003. The dark side of Ras: regulation of apoptosis. Oncogene **22:**8999–9006.
7. **Crul, M., G. J. de Klerk, J. H. Beijnen, and J. H. Schellens.** 2001. Ras biochemistry and farnesyl transferase inhibitors: a literature survey. Anticancer Drugs **12:**163–184.
8. **D'Agostino, D. M., L. Ranzato, G. Arrigoni, I. Cavallari, F. Belleudi, M. R. Torrisi, M. Silic-Benussi, T. Ferro, V. Petronilli, O. Marin, L. Chieco-Bianchi, P. Bernardi, and V. Ciminale.** 2002. Mitochondrial alterations induced by the p13II protein of human T-cell leukemia virus type 1. Critical role of arginine residues. J. Biol. Chem. **277:**34424–34433.
9. **D'Agostino, D. M., L. Zotti, T. Ferro, I. Cavallori, M. Silic-Benussi, L. Chieco-Bianchi, and V. Ciminale.** 2001. Expression and functional properties of proteins encoded in the x-II ORF of HTLV-I. Virus Res. **78:**35–43.
10. **D'Agostino, D. M., L. Zotti, T. Ferro, G. Franchini, L. Chieco-Bianchi, and V. Ciminale.** 2000. The p13II protein of HTLV type 1: comparison with mitochondrial proteins coded by other human viruses. AIDS Res. Hum. Retrovir. **16:**1765–1770.
11. **D'Agostino, D. M., V. Ciminale, L. Zotti, A. Rosato, and L. Chiecobianchi.** 1997. The human T-cell lymphotropic virus type 1 Tof protein contains a bipartite nuclear localization signal that is able to functionally replace the amino-terminal domain of Rex. J. Virol. **71:**75–83.
12. **Dahmoush, L., Y. Hijazi, E. Barnes, M. Stetler-Stevenson, and A. Abati.** 2002. Adult T-cell leukemia/lymphoma: a cytopathologic, immunocytochemical, and flow cytometric study. Cancer **96:**110–116.
13. **Denis, G. V., Q. Yu, P. Ma, L. Deeds, D. V. Faller, and C. Y. Chen.** 2003. Bcl-2, via its BH4 domain, blocks apoptotic signaling mediated by mitochondrial Ras. J. Biol. Chem. **278:**5775–5785.
14. **Derse, D., J. Mikovits, and F. Ruscetti.** 1997. X-I and X-II open reading frames of HTLV-I are not required for virus replication or for immortalization of primary T-cells in vitro. Virology **237:**123–128.
15. **Ding, W., S. J. Kim, A. M. Nair, B. Michael, K. Boris-Lawrie, A. Tripp, G. Feuer, and M. D. Lairmore.** 2003. Human T-cell lymphotropic virus type 1 p12(I) enhances interleukin-2 production during T-cell activation. J. Virol. **77:**11027–11039.
16. **Franchini, G., C. Nicot, and J. M. Johnson.** 2003. Seizing of T cells by human T-cell leukemia/lymphoma virus type 1. Adv. Cancer Res. **89:**69–132.
17. **Gessain, A., R. Mahieux, and T. G. De.** 1996. Genetic variability and molecular epidemiology of human and simian T cell leukemia/lymphoma virus type I. J. Acquir. Immune Defic. Syndr. Hum. Retrovirol. **13**(Suppl. 1)**:**S132–S145.
18. **Gulbins, E., R. Bissonnette, A. Mahboubi, S. Martin, W. Nishioka, T. Brunner, G. Baier, G. Baier-Bitterlich, C. Byrd, and F. Lang.** 1995. FAS-induced apoptosis is mediated via a ceramide-initiated RAS signaling pathway. Immunity **2:**341–351.
19. **Haimovitz-Friedman, A., R. N. Kolesnick, and Z. Fuks.** 1997. Ceramide signaling in apoptosis. Br. Med. Bull. **53:**539–553.

20. **Johnston, S. R.** 2001. Farnesyl transferase inhibitors: a novel targeted therapy for cancer. Lancet Oncol. **2:**18–26.
21. **Kerkhofs, P., H. Heremans, A. Burny, R. Kettmann, and L. Willems.** 1998. In vitro and in vivo oncogenic potential of bovine leukemia virus G4 protein. J. Virol. **72:**2554–2559.
22. **Kimata, J. T., F. Wong, J. Wang, and L. Ratner.** 1994. Construction and characterization of infectious human T-cell leukemia virus type 1 molecular clones. Virology **204:**656–664.
23. **Koralnik, I. J., J. Fullen, and G. Franchini.** 1993. The p12I, p13II, and p30II proteins encoded by human T-cell leukemia/lymphotropic virus type I open reading frames I and II are localized in three different cellular compartments. J. Virol. **67:**2360–2366.
24. **Lefebvre, L., V. Ciminale, A. Vanderplasschen, D. D'Agostino, A. Burny, L. Willems, and R. Kettmann.** 2002. Subcellular localization of the bovine leukemia virus R3 and G4 accessory proteins. J. Virol. **76:**7843–7854.
25. **Lefebvre, L., A. Vanderplasschen, V. Ciminale, H. Heremans, O. Dangoisse, J. C. Jauniaux, J. F. Toussaint, V. Zelnik, A. Burny, R. Kettmann, and L. Willems.** 2002. Oncoviral bovine leukemia virus G4 and human T-cell leukemia virus type 1 p13(II) accessory proteins interact with farnesyl pyrophosphate synthetase. J. Virol. **76:**1400–1414.
26. **Mayo, M. W., J. L. Norris, and A. S. Baldwin.** 2001. Ras regulation of NF-kappa B and apoptosis. Methods Enzymol. **333:**73–87.
27. **Michael, B., A. Nair, and M. D. Lairmore.** 2004. Role of accessory proteins of HTLV-1 in viral replication, T cell activation, and cellular gene expression. Front. Biosci. **9:**2556–2576.
28. **Mortreux, F., A. S. Gabet, and E. Wattel.** 2003. Molecular and cellular aspects of HTLV-1 associated leukemogenesis in vivo. Leukemia **17:**26–38.
29. **Mulloy, J. C., R. W. Crownley, J. Fullen, W. J. Leonard, and G. Franchini.** 1996. The human T-cell leukemia/lymphotropic virus type 1 p12I proteins bind the interleukin-2 receptor beta and gammac chains and affects their expression on the cell surface. J. Virol. **70:**3599–3605.
30. **Nicot, C., M. Dundr, J. M. Johnson, J. R. Fullen, N. Alonzo, R. Fukumoto, G. L. Princler, D. Derse, T. Misteli, and G. Franchini.** 2004. HTLV-1-encoded p30II is a post-transcriptional negative regulator of viral replication. Nat. Med. **10:**197–201.
31. **Pique, C., A. Uretavidal, A. Gessain, B. Chancerel, O. Gout, R. Tamouza, F. Agis, and M. C. Dokhelar.** 2000. Evidence for the chronic in vivo production of human T cell leukemia virus type I Rof and Tof proteins from cytotoxic T lymphocytes directed against viral peptides. J. Exp. Med. **191:**567–572.
32. **Robek, M. D., and L. Ratner.** 2000. Immortalization of T lymphocytes by human T-cell leukemia virus type 1 is independent of the tax-CBP/p300 interaction. J. Virol. **74:**11988–11992.
33. **Robek, M. D., F. H. Wong, and L. Ratner.** 1998. Human T-cell leukemia virus type 1 pX-I and pX-II open reading frames are dispensable for the immortalization of primary lymphocytes. J. Virol. **72:**4458–4462.
34. **Ruvolo, P. P.** 2001. Ceramide regulates cellular homeostasis via diverse stress signaling pathways. Leukemia **15:**1153–1160.
35. **Shi, Y., J. Gera, J. H. Hsu, B. Van Ness, and A. Lichtenstein.** 2003. Cytoreductive effects of farnesyl transferase inhibitors on multiple myeloma tumor cells. Mol. Cancer Ther. **2:**563–572.
36. **Silic-Benussi, M., I. Cavallari, T. Zorzan, E. Rossi, H. Hiraragi, A. Rosato, K. Horie, D. Saggioro, M. D. Lairmore, L. Willems, L. Chieco-Bianchi, D. M. D'Agostino, and V. Ciminale.** 2004. Suppression of tumor growth and cell proliferation by p13II, a mitochondrial protein of human T cell leukemia virus type 1. Proc. Natl. Acad. Sci. USA **101:**6629–6634.
37. **Silverman, L. R., A. J. Phipps, A. Montgomery, L. Ratner, and M. D. Lairmore.** 2004. Human T-cell lymphotropic virus type 1 open reading frame II-encoded p30II is required for in vivo replication: evidence of in vivo reversion. J. Virol. **78:**3837–3845.
38. **Takada, Y., F. R. Khuri, and B. B. Aggarwal.** 2004. Protein farnesyltransferase inhibitor (SCH 66336) abolishes NF-kappaB activation induced by various carcinogens and inflammatory stimuli leading to suppression of NF-kappaB-regulated gene expression and up-regulation of apoptosis. J. Biol. Chem. **279:**26287–26299.
39. **Wrzesinski, S., R. Seguin, Y. Liu, S. Domville, V. Planelles, P. Massa, E. Barker, J. Antel, and G. Feuer.** 2000. HTLV type 1 Tax transduction in microglial cells and astrocytes by lentiviral vectors. AIDS Res. Hum. Retrovir. **16:**1771–1776.
40. **Younis, I., L. Khair, M. Dundr, M. D. Lairmore, G. Franchini, and P. L. Green.** 2004. Repression of human T-cell leukemia virus type 1 and type 2 replication by a viral mRNA-encoded posttranscriptional regulator. J. Virol. **78:**11077–11083.